Available online at www.sciencedirect.com
ScienceDirect
Journal of the European Ceramic Society 27 (2007) 301–306
www.elsevier.com/locate/jeurceramsoc

# Effect of nickel boride additive on simultaneous densification and phase decomposition of $TiB_2$–$WB_2$ solid solutions by pressureless sintering using induction heating

M. Shibuya *, M. Ohyanagi

*Department of Materials Chemistry and HRC, Ryukoku University, Ohtsu 520-2134, Japan*

Received 7 December 2005; received in revised form 26 April 2006; accepted 6 May 2006
Available online 19 June 2006

**Abstract**

Short time process of simultaneous densification and phase decomposition of $TiB_2$–$WB_2$ solid solutions by pressureless sintering using induction heating has been investigated. The products were obtained by sintering of mixture powder compacts of $(Ti,W)B_2$ with nickel and boron (Ni/B = 3/1) varying between 0 and 7.5 wt.%. It was found that the presence of nickel boride as an additive markedly enhances the kinetics of the subsequent densification and decomposition from the $(Ti,W)B_2$ single phase to the two phases of $(Ti,W)B_2$ and $(W,Ti)B_2$. The sintered products were evaluated using X-ray diffraction, scanning electron microscopy, and energy dispersive spectroscopy analysis. In an addition of 7.5 wt.%, the product with a relative density of 91% is produced by induction heating for only 600 s. The mechanical properties of the product, which improved by densification and decomposition of $(Ti,W)B_2$, is also presented.


*Keywords:* Sintering; Composite; Microstructure; Mechanical properties; Borides; $TiB_2$; $WB_2$

## 1. Introduction

Titanium diboride and tungsten diboride are the compound materials with high melting point, hardness, electrical conductivity and thermal conductivity.[1] However, transition metal diborides such as $TiB_2$ and $WB_2$ are difficult for the densification because the dominant mechanism in material transport is evaporation–condensation with no net shrinkage and lower self-diffusivity caused by covalent bonding.[2] On the other aspect, transition metal diborides have the tendency to form extensive solid solutions at high temperatures. The significant thermodynamic property is seen from the subsequent decomposition to two limited solubility phases at low temperatures. The $TiB_2$–$WB_2$ system is a eutectic type as shown in Fig. 1.[3] The solid solutions of $TiB_2$–$WB_2$, that is $(Ti,W)B_2$ phase, has a relatively large region of the solid solution, and $WB_2$ content in $(Ti,W)B_2$ is approximately 63 mol% at eutectic temperature (2230 °C). On the other hand, $(W,Ti)B_2$ has a relatively limited solubility of the solid solution, and $TiB_2$ content in $(W,Ti)B_2$ is approximately 3 mol% at eutectic temperature. In this manner the $(Ti,W)B_2$ solid solutions can be decomposed to the two phases of $(Ti,W)B_2$ and $(W,Ti)B_2$ by heat treatment, and the phase decomposition can be used to control the microstructure.[3] The microstructural control can improve the mechanical properties such as the fracture toughness.

Solid solutions of $TiB_2$–$WB_2$ have been produced by annealing mixtures of two borides, a process that requires high temperatures (∼2000 °C) and long times (∼8 h).[4,5] In previous studies, the formation of the $TiB_2$–$WB_2$–$CrB_2$ solid solutions by field activation using the spark plasma sintering (SPS) apparatus has been investigated.[6] In that method, synthesis was conducted using elemental reactants, reacted under the influence of a high, pulsed dc current and a uniaxial pressure. With that approach, 94% dense $(Ti,W,Cr)B_2$ phase was formed by reacting the powders at 1900 °C for 10 min. The decomposition of those solutions to two phases has been found to be kinetically slow.

In a recent investigation,[7] the present authors produced the $TiB_2$–$WB_2$ solid solutions by induction field activated com-

* Corresponding author at: AIST (National Institute of Advanced Industrial Science and Technology), 1-1-1 Higashi, Tsukuba, Ibaraki 305-8565, Japan. Tel.: +81 29 861 4410; fax: +81 29 861 4410.
*E-mail address:* m-shibuya@aist.go.jp (M. Shibuya).

0955-2219/$ – see front matter © 2006 Elsevier Ltd. All rights reserved.
doi:10.1016/j.jeurceramsoc.2006.05.081

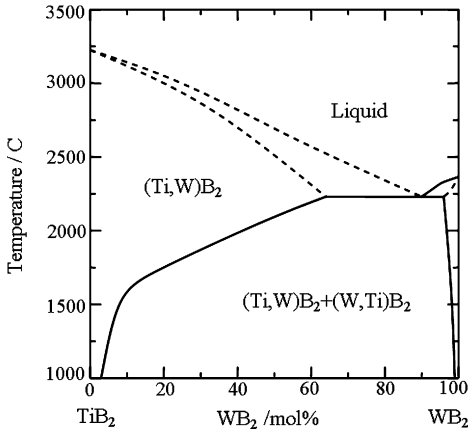


Fig. 1. Quasi-binary phase diagram of $TiB_2$–$WB_2$ system: after Ref.[3].

bustion synthesis (IFACS)[8,9] for 2 min, using elemental reactants. Moreover, nickel or cobalt, which are known as the additive agent of pressureless sintering of $TiB_2$,[10–14] was added in $(Ti,W)B_2$ for simultaneous sintering and phase decomposition of the solid solutions produced by the IFACS method.[15] The phase decomposition occurred within 360 s by induction heating, however, the products were not dense bodies. Therefore, other additive agent needed for the densification with the phase decomposition.

In the present work, we investigate the effect of the addition of nickel boride on simultaneous densification and phase decomposition of the $TiB_2$–$WB_2$ solid solutions formed by the IFACS method. The addition of boride with low melting point such as nickel boride or cobalt boride leads to the densification by liquid phase sintering because the pseudo-binary eutectic reaction occurs at relatively low temperature.[16–19]

## 2. Experimental procedure

High-purity powders of Ti, W and B were used as reactants in this study. The titanium powder is 99.5% pure and has an average particle size of about 22 μm (Sumitomo Sitix, Inc., Amagasaki, Japan). The tungsten powder is 99.9% pure with an average particle size of about 8 μm and the crystalline boron powder is 99% pure with a particle size of less than 45 μm. The additive powder is 99.9% pure nickel with a particle size of about 2–3 μm. The W, B and Ni powders were obtained from Kojundo Chemical Laboratory, Inc. (Sakaido, Japan). Powders of titanium, tungsten and boron were weighed out in mole ratios of Ti/W/B = 6/4/23 to give a composition of $6TiB_2$–$4WB_2$ solid solution and were dry-mixed in an automatic agate mortar for 1 h. Excess boron was used because of previous experience indicating the loss of this element (due to the evaporation of its oxide) during synthesis.[7]

The mixed powders were packed into a cylindrical carbon sheet, 0.7 mm in thickness and 40 mm in diameter and 10 mm long. The packing density of each powder compact is about 50%. Each sample was placed in commercial casting sand inside a silicon nitride crucible of 70 mm in inside diameter, 140 mm in outside diameter and 70 mm in depth. That crucible was placed in the IFACS equipment.[7] Detail of the experimental setup was provided in previous publications.[7–9] The reaction in the sample was ignited by induction under the conditions of 85 V, 170 A, 70 kHz and 120 s. The powders of resulting $(Ti,W)B_2$ phase ($TiB_2/WB_2$ = 6/4) were crushed by ball milling using silicon nitride jar and balls until an average particle size of 2 μm was obtained.

Heat treatment by induction heating was conduced for sintering and decomposition of the solid solutions. To the powder of $(Ti,W)B_2$ phase, the powder in mole ratios of Ni/B = 3/1 ($Ni_3B$) was added at levels from 0 to 7.5 wt.%, and was dry-mixed in an automatic agate mortar for 30 min. From these mixed powders, cylindrical compacts, about 16 mm in diameter and 10 mm long were formed by cold isostatic pressing at 250 MPa. The packing density of the powder compact is about 60%. The powder compact was placed in a cylindrical carbon sheet, about 47 mm in diameter and 17 mm long. The carbon crucible with the compact was placed in commercial casting sand inside the silicon nitride crucible described above. The heat treatment was performed by induction heating (85 V, 170 A, 70 kHz) under atmospheric pressure of air. The sample, being embedded in the carbon sheet, experienced a reducing environment.

The sample temperatures were measured with W–$Re_{5\%}$/W–$Re_{26\%}$ thermocouples using a data acquisition recorder as described in previous publications.[7–9] The products were analyzed by X-ray diffraction (RINT2500: RAD-C system, Rigaku Inc., Tokyo, Japan) using Cu Kα radiation. Microstructural and elemental analyses were conducted on cross-sections of the annealed samples using scanning electron microscopy (SEM) and energy dispersion spectroscopy (EDS) (JSM-330; JEOL Inc., Tokyo, Japan). The density of the products was measured by the Archimedes method. The hardness of each product was determined by the Vickers micro-hardness apparatus (HMV-2000, Shimazu Inc., Kyoto, Japan) at 0.98 N force for 10 s. The fracture toughness of the products was determined by indentation crack measurements[20] using the Vickers hardness at 19.6 N force for 10 s. The cracks developed at the corners of the Vickers hardness indentation were used to measure the surface critical stress intensity factor $K_{IC}$.

## 3. Results and discussion

Pressureless sintering was performed by induction heating under atmospheric pressure for simultaneous densification and decomposition of $(Ti,W)B_2$ phase with a $WB_2$ composition of 40 mol%. A typical temperature profile of a sample, the solid solution with 7.5 wt.% $Ni_3B$, heated by induction current through carbon sheets is shown in Fig. 2. The temperature increases at a heating rate of 700 °C $min^{-1}$ in the initial stage. Endothermic reaction at 1156 °C corresponds to the melting point of $Ni_3B$. And then the temperature increases smoothly to a maximum of 1940 °C after 350 s. The temperature was then held constant for an additional 250 s. As shown in the phase diagram of Fig. 1, the decomposition of the $(Ti,W)B_2$ phase with a $WB_2$ composition of 40 mol% easily occurs at 1940 °C.

Fig. 3 shows the effect of $Ni_3B$ addition at a sintering time of 600 s and induction heating time in sample containing 7.5 wt.% $Ni_3B$ on the volume shrinkage of the samples, which occurred by

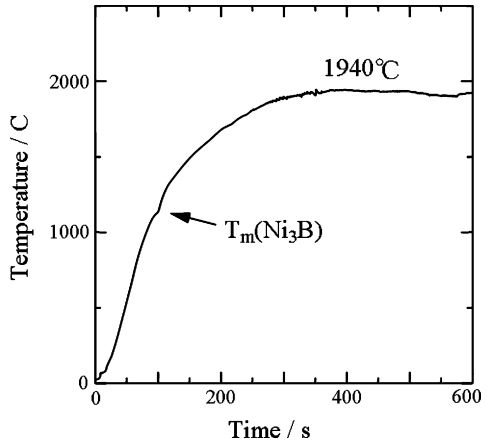


Fig. 2. Temperature profile of the sample under induction heating ($(Ti,W)B_2$–7.5 wt.% $Ni_3B$).

induction heating. The volume shrinkage increases with $Ni_3B$ addition and is almost saturated when the additive amount is higher than 5 wt.%. The volume shrinkage for a sample which contained 7.5 wt.% $Ni_3B$ is about 28%. As shown in an inset figure, the volume shrinkage gradually increases with induction heating time until 600 s. It indicates that the sample was sintered under a raising temperature for 350 s and a holding temperature of 1940 °C for 250 s as shown in Fig. 2.

X-ray diffraction patterns of the products sintered by induction heating for 600 s are shown in Fig. 4. The patterns show the products which contained $Ni_3B$ of (a) 0 wt.%, (b) 2.5 wt.%, (c) 5.0 wt.% and (d) 7.5 wt.%. The peaks of the product without addition are those belonging to the $(Ti,W)B_2$ phase which corresponded closely to the diffraction peaks of $TiB_2$ (hexagonal $AlB_2$ structure, *P6/mmm*) and β-(W,Ti)B which corresponded closely to the diffraction peaks of β-WB (orthorhombic structure, *Cmcm*) as a minor impurity. The precipitation of β-WB phase has been also reported on sintering of the

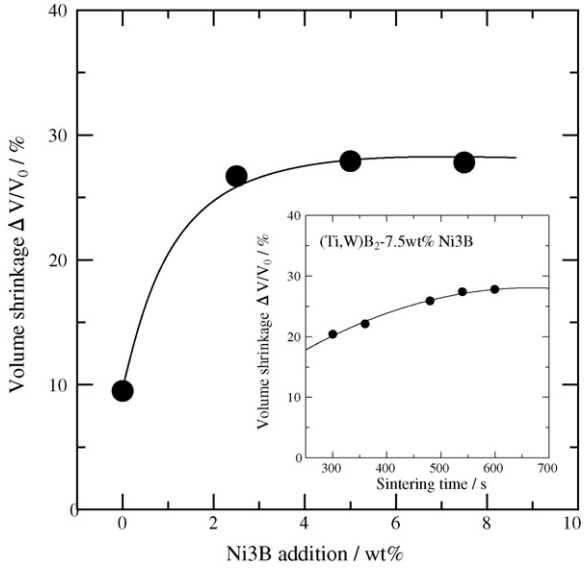


Fig. 3. Effect of $Ni_3B$ addition and induction heating time on the volume shrinkage of the products.

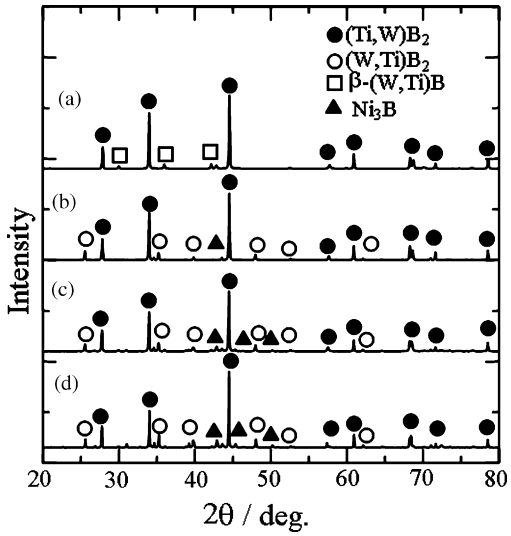


Fig. 4. X-ray diffraction patterns of the products sintered by induction heating for 600 s: (a) 0 wt.%, (b) 2.5 wt.%, (c) 5.0 wt.% and (d) 7.5 wt.% $Ni_3B$ addition.

$TiB_2$–$CrB_2$–$WB_2$ solid solutions.[5,6] In contrast, the patterns of the products with the $Ni_3B$ additives contain the diffraction peaks belonging to $(Ti,W)B_2$, $(W,Ti)B_2$ which has the hexagonal $W_2B_5$ structure (*P6*$_3$*/mmc*) and $Ni_3B$ as a minor impurity. The peak intensity of $(W,Ti)B_2$ increases with amount of the addition. The XRD peaks of the products with the addition show a shift to lower $2\theta$ values for the (0 0 1) peak (at $2\theta = 28.0$ for the sample without addition) as well as in the case of the Ni or Co addition.[15] In view of the dependence of the lattice parameters on the composition in the solid solution,[7,15,21] this observation is consistent with the decrease in W content of the solid solution as a result for the precipitation of the second phase. Results for EDS analyses on the $(Ti,W)B_2$ and $(W,Ti)B_2$ phases indicated that the former contained less tungsten than the solid solution without addition. For a solid solution with a composition of 40 mol% $WB_2$, in the case of an addition of 7.5 wt.%, the concentration of W in $(Ti,W)B_2$ after decomposition is equivalent to less than 20 mol% $WB_2$. The decomposition time is very short by the $Ni_3B$ addition as well as in the case of the Ni or Co addition,[15] compared with the previous works which required annealing for 2 h at 1600 °C[5] and 14 h at 1500 °C.[6] It can be explained that the reason of the decomposition accelerated by the addition of $Ni_3B$ is influence of boron transfer enhanced in molten Ni or $Ni_3B$. That is, the decomposition occurs by transfer of the boron atoms. EXAFS (extended X-ray absorption fine structure) studies on $(Ti,W)B_2$ composites[3] indicated that a high amount of the boron atoms is transferred from near titanium environment to a tungsten neighborhood during high temperature treatment.

The microstructure morphology of the products changed with the $Ni_3B$ additions. Scanning electron micrographs (backscattered electron images) of cross-section of the products sintered by induction heating for 600 s are shown in Fig. 5. Identification of the phases was performed by EDS. Ti/W mole ratios obtained by EDS measurement indicate on the photographs. It is clear that the darker gray phase and the lighter gray phase are $(Ti,W)B_2$ and $(W,Ti)B_2$, respectively. W mole ratio dras-

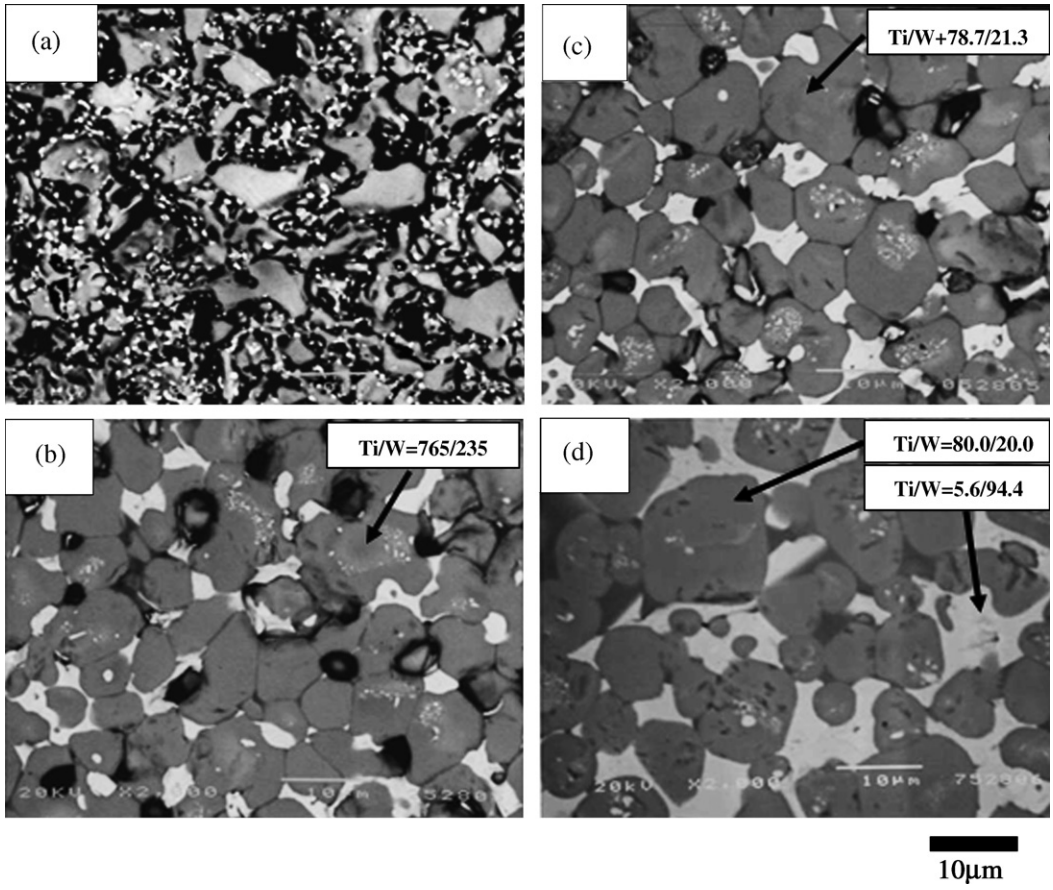


Fig. 5. Scanning electron micrographs of cross-section of the products sintered by induction heating for 600 s: (a) 0 wt.%, (b) 2.5 wt.%, (c) 5.0 wt.% and (d) 7.5 wt.% $Ni_3B$ addition.

tically decreased by the decomposition. W mole ratio of the lighter gray phase, which shown in Fig. 5(d), is higher than that of $(W,Ti)B_2$ as shown in the phase diagram (Fig. 1). Because a small amount of $(Ti,W)B_2$ was contained in the lighter gray phase. In the product without the addition, Fig. 5(a) presents porous structure and small particles of white color are seen. The small particles with the size of submicron are β-(W,Ti)B precipitated in the grain boundary as identified in XRD pattern of Fig. 4(a). The small particles of β-(W,Ti)B would be the trace of the $(W,Ti)B_2$ seed crystals. Fig. 5(b)–(d) shows the presence of the two phases $(Ti,W)B_2$ and $(W,Ti)B_2$. The densification enhances with increasing $Ni_3B$ addition, and the product in a $Ni_3B$ addition of 7.5 wt.% is dense body without pores. $Ni_3B$ shown in XRD patterns is also observed in the grain boundary between the $(Ti,W)B_2$ and $(W,Ti)B_2$ phases. The precipitation of $Ni_3B$ has been previously reported as a major secondary phase during sintering of $TiB_2$ with nickel as a sintering aid.[10,14] The $(W,Ti)B_2$ phases precipitated in the grain boundary of the $(Ti,W)B_2$ phases generally have platelet shape,[4,5,15] however, the $(W,Ti)B_2$ grains in this study have round shape produced from the liquid phases. This result indicates that the sintering temperature is lower than the melting temperature of $(Ti,W)B_2$ and $(W,Ti)B_2$, however, the melting temperature of the solid solutions have been decreased by pseudo-binary eutectic reaction between the solid solutions and $Ni_3B$. That is, $Ni_3B$ was dissolved into the near surface of the particles of the solid solutions, and the eutectic temperature between $Ni_3B$ and the solid solutions would be decreased to lower than the sintering temperature. Therefore, this phenomenon leads to an enhancement of the densification by liquid phase sintering. Related to this proposed explanation has been finding that a CoB addition of 1.0 wt.% markedly enhances the densification of $TiB_2$,[22] and N–B coated WC powders easily leads to liquid phase sintering.[17]

The effect of $Ni_3B$ addition on the bulk density and relative density of the products sintered by induction heating for 600 s is shown in Fig. 6. The density of the products increases with amount of the addition. The density in an addition of 7.5 wt.% is 7.01 g $cm^{-3}$, corresponds to 91% of the theoretical value, as calculated from the lattice constants determined by the XRD measurement and results for the ESD analyses. In the previous study, the solid solutions of $TiB_2$–$WB_2$–$CrB_2$ system with high densities as high as 94% has been obtained using spark plasma sintering (SPS).[6] By that method, the consolidation simultaneously occurred with the reaction to form the solid solution from the elemental reactants, however, an applied pressure of 64 MPa was required.

The mechanical properties of the products were improved by $Ni_3B$ additions. Precipitated $Ni_3B$ is brittle phase.[10] However, the mechanical properties greatly depend on the densification and phase decomposition. Table 1 shows the Vickers micro-

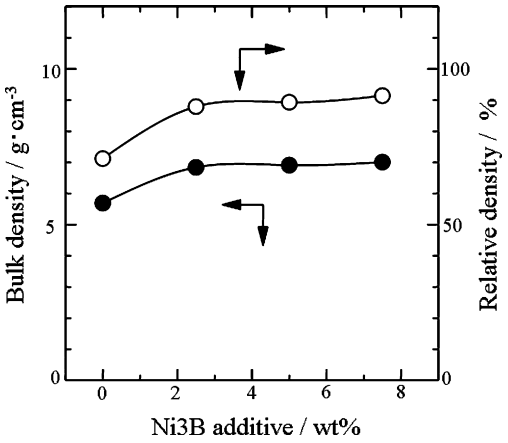


Fig. 6. Effect of $Ni_3B$ addition on the bulk density and relative density of the products sintered by induction heating for 600 s.

Table 1
Vickers microhardness and fracture toughness of the product in this work and $TiB_2$ based composite

| | Vickers microhardness (GPa) | Fracture toughness, $K_{IC}$ (MPa m$^{1/2}$) | Reference |
|---|---|---|---|
| (Ti,W)$B_2$–7.5 wt.%$Ni_3B$ | 20.0 ± 1.4 | 7.9 ± 0.6 | |
| $TiB_2$–(Fe–Ni) | 20.0 ± 1.0 | 8.2 ± 0.3 | 23 |
| $TiB_2$–TiN | 21.8 | 5.1 | 24 |
| (Ti,W,Cr)$B_2$ | 22.7 | – | 6 |

hardness and the fracture toughness of the product obtained in this work and the literature values. The fracture toughness in all cases was determined by indentation crack measurements. About the literature values, the $TiB_2$ base cermet were produced by hot isostatic pressing at 1350 °C and 150 MPa for 30 min,[23] the $TiB_2$–TiN nonocomposite were produced by SPS at 70 MPa for 12 min,[24] and the dense (Ti,W,Cr)$B_2$ phase were formed by SPS at 64 MPa for 10 min.[6] The Vickers microhardness and fracture toughness $K_{IC}$ of the product obtained in this work are approximately 20.0 GPa and 7.9 MPa m$^{1/2}$, respectively. In spite of pressureless sintering for 10 min, these values almost correspond to the literature values because of the densification and phase decomposition prevented the particle cohesion of the (Ti,W)$B_2$ phase.

## 4. Conclusion

The effect of nickel boride additive on the simultaneous densification and phase decomposition of the $TiB_2$–$WB_2$ solid solutions, with a $WB_2$ content of 40 mol%, by induction heating under pressureless was investigated. The densification and phase decomposition are enhanced by the addition of nickel boride. With an addition of 7.5 wt.% $Ni_3B$, the product obtained by induction heating for 600 s has dense body with the two (Ti,W)$B_2$ and (W,Ti)$B_2$ phases, and the relative density is 91%. The Vickers microhardness and the fracture toughness $K_{IC}$ of the product are 20.0 GPa and 7.9 MPa m$^{1/2}$, respectively. The formation of nickel boride is suggested as playing a role in the enhancement of the densification and decomposition of the solid solutions.

## Acknowledgement

The authors are grateful to Dr. E. Akiba (National Institute of Advanced Industrial Science and Technology) for providing support.

## References

1. Castaing, J. and Costa, P., In *Boron and Refractory Boride*, ed. V. I. Matkovich. Springer-Verlag, Berlin, Heidelberg, New York, 1977. p. 390.
2. Ouabdesselam, M. and Munir, Z. A., The sintering of combustion-synthesized titanium diboride. *J. Mater. Sci.*, 1987, **22**, 1799–1807.
3. Pohl, A., Telle, P. and Aldinger, F., EXAFS studies of (Ti,W)$B_2$ compounds. *Z. Metallkd.*, 1994, **85**, 658–663.
4. Telle, R., Fendler, E. and Petzow, G., The quasi-binary systems $CrB_2$–$TiB_2$, $CrB_2$–$WB_2$ and $TiB_2$–$WB_2$. *J. Hard Mater.*, 1992, **3**, 211–224.
5. Mitra, I. and Telle, R., Phase formation during anneal of supersaturated $TiB_2$–$CrB_2$–$WB_2$ solid solutions. *J. Solid State Chem.*, 1997, **133**, 25–30.
6. Kaga, H., Carrillo-Heian, E. M., Munir, Z. A., Schmalzried, C. and Telle, R., Synthesis of hard materials by field activation: the synthesis of solid solutions and composites in the $TiB_2$–$WB_2$–$CrB_2$ system. *J. Am. Ceram. Soc.*, 2001, **84**(12), 2764–2770.
7. Shibuya, M., Kawata, M. and Ohyanagi, M., Titanium diboride–tungsten diboride solid solutions formed by induction-field-activated combustion synthesis. *J. Am. Ceram. Soc.*, 2003, **85**, 706–710.
8. Ohyanagi, M., Hiwatashi, T., Koizumi, M. and Munir, Z. A., Induction field activated SHS compaction. In *Proceedings of the First Russian-Japanese Workshop SHS*, 1998, pp. 65–69.
9. Kata, D., Ohyanagi, M. and Munir, Z. A., Induction-field-activated self-propagating high-temperature synthesis of AlN–SiC solid solutions in the $Si_3N_4$–Al–C system. *J. Mater. Res.*, 2000, **15**, 2514–2525.
10. Ferber, M., Becher, P. and Finch, C., Effect of microstructure on the properties of $TiB_2$ ceramics. *J. Am. Ceram. Soc.*, 1983, C2–C4.
11. Graziani, T., Bellosi, A. and Fabbriche, D. D., Effects of some iron-group metals on densification and characteristics of $TiB_2$. *Refract. Met. Hard Mater.*, 1992, **11**, 105–112.
12. Hoke, D. A. and Meyers, M. A., Consolidation of combustion-synthesized titanium diboride-based materials. *J. Am. Ceram. Soc.*, 1995, **78**, 275–284.
13. Kim, W. J., Kim, D. H., Kang, E. S., Kim, D. K. and Kim, C. H., Two-step sintering of a $TiB_2$–Ni cermet. *J. Mater. Sci.*, 1996, **31**, 5805–5809.
14. Einarsrud, M., Hagen, E., Pettersen, G. and Grande, T., Pressureless sintering of titanium diboride with nickel, nickel boride, and iron additives. *J. Am. Ceram. Soc.*, 1997, **80**, 3013–3020.
15. Shibuya, M., Yoneda, T., Yamamoto, Y., Ohyanagi, M. and Munir, Z. A., Effect of Ni and Co additives on phase decomposition in $TiB_2$–$WB_2$ solid solutions formed by induction field activated combustion synthesis. *J. Am. Ceram. Soc.*, 2003, **86**, 354–356.
16. Watanabe, T. and Kouno, S., Mechanical properties of $TiB_2$–CoB–metal boride alloys. *Ceram. Bull.*, 1982, **61**, 970–973.
17. Vélez, M., Quiñones, H., Di Giampaolo, A. R., Lira, J. and Grigorescu, I. C., Electroless Ni–B coated WC and VC powders as precursors for liquid phase sintering. *Int. J. Refract. Met. Hard Mater.*, 1999, **17**, 99–102.
18. Özkan Gülsoy, H., Influence of nickel boride additions on sintering behaviors of injection moulded 17-4 PH stainless steel powder. *Scripta Mater.*, 2005, **52**, 187–192.
19. Jung, J. and Kang, S., Microstructure of TiC–TiN–Ni–(B) cermet systems. *Powder Metall.*, 2002, **45**, 83–89.
20. Lawn, B. R. and Fuller, E. R., Equilibrium penny-like cracks in indentation fracture. *J. Mater. Sci.*, 1975, **10**, 2016–2024.

21. Kuz'ma, Y. B., Svarichevskaya, S. I. and Telegus, V. S., Systems titanium–tungsten–boron, hafnium–tantalum–boron, and tantalum–tungsten–boron. *Sov. Powder Metall. Met. Ceram.*, 1971, **10**, 478–481.
22. Watanabe, T., Miura, H. and Tokunaga, Y., Densification mechanism of $TiB_2$–1% CoB and $TiB_2$–5% $TaB_2$–1% CoB systems. *J. Jpn. Soc. Powders Powder Metall.*, 1986, **33**, 38–42.
23. Sanchez, J. M., Azcona, I. and Castro, F., Mechanical properties of titanium diboride based cermets. *J. Mater. Sci.*, 2000, **35**, 9–14.
24. Lee, J. W., Munir, Z. A., Shibuya, M. and Ohyanagi, M., Synthesis of dense $TiB_2$–TiN nanocrystalline composites through mechanical and field activation. *J. Am. Ceram. Soc.*, 2001, **84**, 1209–1216.